RAFFLES BULLETIN OF ZOOLOGY **74**: 606–623
Date of publication: 24 July 2026
DOI: 10.26107/RBZ-2026-0038
https://zoobank.org/urn:lsid:zoobank.org:pub:4D154D3B-2BA7-4875-A1E2-96EEA01966C6

Nanosphronemus gemma, a remarkable new genus and species of miniature osphronemid from Vietnam (Teleostei: Anabantoidei: Osphronemidae)

Ralf **Britz**[1*], Heok Hui **Tan**[2] & Lukas **Rüber**[3,4]

Abstract. A new genus and species of miniature labyrinth fish of the family Osphronemidae, *Nanosphronemus gemma*, is described from Vietnam. It differs from all other genera of anabantoids by a unique dorsal- and anal-fin ray count, a unique colour pattern and a number of unique or highly unusual skeletal characters. Our molecular phylogenetic analysis indicates that *Nanosphronemus* is the sister group of the genus *Trichopsis*, the croaking gouramis.

Key words. Anabantoidei, labyrinth fishes, miniaturisation, gourami

INTRODUCTION

The labyrinth fishes of the suborder Anabantoidei comprise around 170 species distributed in freshwaters in Africa and Asia (Norris & Teugels, 1990; Kottelat, 2013; Skelton et al., 2021; Fricke et al., 2026). Anabantoidei are divided into three families, the Afro-Asian Anabantidae with 33 species, the monotypic Southeast Asian Helostomatidae, and the Asian Osphronemidae, the most species-rich family with 137 species. Anabantoidei are characterised by an accessory airbreathing organ, the so-called suprabranchial organ or labyrinth organ, which is housed in a suprabranchial cavity above the gill arches (Henninger, 1908; Bader, 1937; Liem, 1963, 1980; Peters, 1978). It consists of a modified epibranchial 1 with a complex system of membrane bone extensions which, in its most complicated form, resembles a labyrinth (e.g., in *Osphronemus*, see Peters, 1978). The epithelium of this modified epibranchial 1, as well as that of the cavity, is heavily invested with blood vessels, which aid in taking up oxygen from the air that is swallowed into the suprabranchial cavity (Henninger, 1908; Liem, 1963, 1980; Peters, 1978). The labyrinth organ has enabled members of the Anabantoidei to conquer habitats with low oxygen content, especially swamp areas.

Accepted by: Kevin W. Conway

[1]Senckenberg Natural History Collections Dresden, Museum of Zoology, DE-01109 Dresden, Germany. E-mail: ralf.britz@senckenberg.de (*corresponding author)

[2]Lee Kong Chian Natural History Museum, National University of Singapore, 2 Conservatory Drive, Singapore 117377. E-mail: heokhui@nus.edu.sg

[3]Naturhistorisches Museum Bern, 3005 Bern, Switzerland

[4]Aquatic Ecology and Evolution, Institute of Ecology and Evolution, University of Bern, 3012 Bern, Switzerland

ISSN 2345-7600 (electronic) | ISSN 0217-2445 (print)

Anabantoids have been the subject of phylogenetic studies starting with Liem's (1963) monographic treatment and several subsequent papers (Liem, 1965, 1967a, 1967b). Britz (1994), Britz et al. (1995), Britz (2001), Britz & Cambray (2001), and Rüber et al. (2006) provided significant changes to the phylogenetic relationships of anabantoids on which the current classification is based.

The distribution of the most species-rich family, the Osphronemidae, extends in Asia from the Indus in Pakistan in the West to Sri Lanka in the Southwest, to the Amur basin in China in the East, and to the Sunda Islands in the Southeast. The included 14 genera are assigned to five subfamilies (Britz, 1994; Britz et al., 1995; Britz, 2001; Britz & Cambray, 2001; Rüber et al., 2006): (1) the Belontiinae with the single genus *Belontia*, (2) the Osphroneminae, with the genus *Osphronemus*, (3) the Luciocephalinae with *Luciocephalus*, *Sphaerichthys*, *Parasphaerichthys*, and *Ctenops*, (4) the Trichogastrinae with *Trichogaster* and *Trichopodus*, and (5) the Macropodusinae with *Macropodus*, *Pseudosphromenus*, *Malpulutta*, *Trichopsis*, *Betta*, and *Parosphromenus*.

Recently, a miniature labyrinth fish was discovered in Central Vietnam, and has been subsequently available in the aquarium trade. We used the opportunity to describe this remarkable new species of anabantoid and comment on its anatomy and phylogenetic relationships.

MATERIAL AND METHODS

Morphological methods. Measurements were taken from point to point with digital callipers to the nearest 0.1 mm. Due to their tiny size, the specimens were difficult to handle and measure; therefore, only measurements that could be taken reliably were recorded.

To count vertebrae and dorsal-, anal-, and caudal-fin rays, 15 specimens of *Nanosphronemus gemma* and another 24 members of the suborder Anabantoidei covering all genera except *Sandelia* were radiographed. Two specimens of *N. gemma* (female 16.1 mm SL, male 16.2 mm SL) were CT-scanned with a Zeiss X-Radia Context with a voxel size of 4.5 or 4.76 for the body and 3.8 or 3.57 for the head, with an exposure of 2–3 sec. and 2–3 frames and 1,401 to 1,801 projections and with no filter. CT scan data were segmented in Dragonfly® and then segmented volumes were rendered and imaged in Amira®. Vertebral and dorsal- and anal-fin ray counts for the type series of *N. gemma* and additional anabantoids were taken from digital radiographs. Additional counts came from the two CT scanned non-types of *Nanosphronemus* (MTD 40216). Pectoral-fin ray counts on alcohol-preserved specimens are difficult to obtain; the recorded 10–11 rays may be one or two rays too low, as the CT-scanned specimens, which allowed for accurate counts, had 12 and 13 rays. We use the term miniature for tiny-sized fishes as defined by Weitzman & Vari (1988).

Molecular methods. To place *Nanosphronemus* into a larger molecular phylogenetic framework we sequenced the complete mitochondrial cytochrome b (cytb), partial 12S rRNA, complete tRNA Val, and partial 16S rRNA genes as well as the partial nuclear RAG1 gene of one specimen. The newly generated sequences were integrated into a previously published data set for the molecular phylogenetics of labyrinth fishes (Rüber et al., 2006). Laboratory procedures including DNA extraction from tissues preserved in 100% EtOH and PCR amplification of *Nanosphronemus* followed protocols by Rüber et al. (2006) using the PCR primers described in Rüber et al. (2023). Additionally, we also sequenced the DNA barcoding gene cytochrome oxidase I (COI) for the same individual following Rüber et al. (2023). PCR products were cleaned and Sanger sequenced, using the same primer pairs that were used for the PCR amplification. Raw reads were edited and assembled into contigs using Geneious Prime v2026.0.2 (https://www.geneious.com). For the phylogenetic data set, the individual consensus sequences were aligned using MAFFT v7.490 (Katoh & Standley, 2013), together with previously published sequences (Rüber et al., 2006) in Geneious Prime. The COI sequence of one specimen of *Nanosphronemus*, generated for this study, was aligned with COI sequences of labyrinth fishes obtained from GenBank and BOLD.

Gaps and alignment ambiguities in the 12S rRNA-tRNA Val-16S rRNA alignment were excluded using GBlocks (Castresana, 2000) as implemented in NGPhylogeny.fr (Lemoine et al., 2019) using default parameters. Maximum likelihood (ML) analyses with 1,000 ultrafast bootstrap replicates were conducted for the combined cytb, 12S rRNA-tRNA Val-16S rRNA, and RAG1 data set using IQ-TREE v2.3.644 (Minh et al., 2020) and an initial partition scheme by gene and codon position (e.g., cytb first, second and third codon position, RNA, and RAG1 first, second and third codon position) using the model option "-m MFP+MERGE" and results were visualised in FigTree v1.4.4 (http://tree.bio.ed.ac.uk/software/Figtree/). Genetic distances (uncorrected p-distances) between *Nanosphronemus* and selected labyrinth fish genera for COI were calculated in PAUP* v4.0a147 (Swofford, 2002).

Nanosphronemus, new genus

(Figs. 1–11)

Diagnosis. *Nanosphronemus* differs from all other genera in the suborder Anabantoidei by its unique count of XIX–XXI+2–3 dorsal-fin rays (vs. I–XVIII+ 4–14, rarely XIX in some specimens of *Macropodus ocellatus*) and XX–XXIV+4–5 anal-fin rays (vs. I–XVII+8–38, rarely XX–XXII in some specimens of *Macropodus* spp.), the presence (vs. absence) of a series of anteroventrally directed processes off the distal part of caudal haemal arches, Baudelot's ligament inserting on the exoccipital (vs. on basioccipital, first or second vertebra), and a unique colour pattern in sexually active males consisting of a dark-brown to black mid-lateral stripe with numerous bluish-green iridescent scales and a blood-red stripe above it, running from behind the posterior margin of the eye onto the base of the caudal fin (vs. different colour pattern). *Nanosphronemus* differs from all anabantoid genera except *Helostoma* in the absence (vs. presence) of the exoccipital foramen and from all anabantoid genera except *Trichogaster*, *Trichopodus*, *Ctenops*, *Parasphaerichthys*, *Sphaerichthys*, and *Luciocephalus* in having only five (vs. six) branchiostegal rays. An additional diagnostic, though not exclusive, character is the miniature size in *Nanosphronemus* of under 19 mm SL, only shared with *Parasphaerichthys lineatus* (Britz & Kottelat, 2002).

Etymology. The new genus name is derived from the Ancient Greek word, νάνος, meaning dwarf, combined with the name *Osphronemus*, the type genus of the family Osphronemidae, to which this new genus belongs. Gender: masculine. The name alludes to the tiny size of this new fish, which makes it one of the smallest anabantoids known to date.

Type species. *Nanosphronemus gemma*, new species

Nanosphronemus gemma, new species

(Figs. 1–11)

Holotype. ZRC 70244, 18.7 mm SL, Central Vietnam, reportedly from wetlands of an undisclosed area in the vicinity of Huế.

Paratypes. ZRC 70070, 14 ex., 14.6–18.3 mm SL, same information as for holotype.

Additional non-type material. MTD 40216, 2, 16.2–16.4 mm SL, same information as holotype.

Suggested common name. Jewel Gourami.

Diagnosis. See diagnosis of genus.

Description. For general appearance, see Figs. 1–3. Miniature anabantoid, with a maximum size of 18.7 mm. Elongate body, circular in cross section at head, slightly laterally

Fig. 1. *Nanosphronemus gemma*, holotype, ZRC 70244, 18.7 mm SL, in lateral view.

compressed to oval cross section behind head, but more laterally compressed in posterior third of body. Head large, almost one-third of standard length. Mouth small, superior; snout short. Eye very large, more than one-third of head length. Dorsal profile rising sharply from tip of mouth to nape with concave depression between mouth and interorbital area; dorsal profile continuing almost in a straight line, then descending gradually to caudal peduncle. Ventral profile descending sharply from snout to jaw articulation, then more gradually to pectoral area, more or less horizontal between pelvic-fin base and middle of anal fin, from there ascending gradually to caudal peduncle. Dorsal and anal fins very long, reaching 50–60% of standard length. Dorsal fin with 19–21 fin spines and 2–3 rays, anal fin with 21–24 spines and 4–5 rays. Pectoral fin with usually 11, rarely 10 rays (but see Methods). Pelvic fin inserted below base of pectoral fin, with one spine and five rays, the first four branched. Caudal fin rounded, with one dorsal and two ventral procurrent rays and 6+6 principal rays.

Body and head except mouth region scaled (Fig. 4–5); body mostly with transforming ctenoid scales with up to four series of cteni; cteni missing from scales covering head dorsally, laterally and ventrally (Fig. 5) and also missing from scales on dorsum along dorsal fin and ventrally from shoulder girdle along anal fin base (Fig. 4), so that scales appear cycloid. 28–29 scales in a lateral series, four to five scales between lateral series and dorsal-fin base and five to six scales between lateral series and anal-fin base. Base of dorsal- and anal-fin spines covered by series of small elongate, cycloid scales. Basal fourth of caudal fin also covered by small and thin cycloid scales. Lateral-line canal restricted to head; no perforated lateral-line scales on body. Only three lateral-line pores associated with frontal, three with extrascapular, none with pterotic, two with lachrymal, and five with preopercle (Fig. 5).

Suprabranchial chamber extending posteriorly to level of third vertebra (Fig. 6), housing simplified labyrinth organ formed from modified epibranchial 1.

Colouration in preservative. After formalin preservation (Fig. 1), body colouration cream with two stripes; mid-lateral stripe black, 1½ scales wide, extending from snout through middle of eye posteriorly to base of lower half of caudal fin forming lower caudal-fin spot; dorsolateral stripe, lighter, brown or reddish brown, ½ to 1 scale wide, extending from dorsoposterior corner of opercle to upper half of caudal fin forming fainter upper caudal fin spot.

Table 1. Morphometric information for holotype (ZRC 70244) and nine paratypes (ZRC 70070) of *Nanosphronemus gemma*.

	N=10 (holotype)
Standard length (SL) in mm	15.3–18.7 (18.7)
In percent of SL	
Predorsal length	38.2–43.4 (38.5)
Caudal-peduncle depth	11.8–14.2 (11.8)
Preanal length	40.4–48.4 (41.7)
Head length (HL)	25.7–32.2 (28.9)
Dorsal-fin depth	24.6–28.1 (24.6)
Pelvic-fin length	16.0–21.3 (16.0)
Anal-fin base length	52.9–59.6 (52.9)
Dorsal-fin base length	50.8–59.9 (50.8)
In percent of HL	
Orbit diameter	33.3–41.7 (37.0)
Postorbital length	45.5–54.2 (48.1)
Interorbital width	24.1–30.8 (24.1)
Snout length	14.8–22.2 (14.8)

Two specimens selected for CT-scanning and preserved in ethanol with much darker overall colouration than formalin preserved specimens (Fig. 2). Female (MTD 40216, identified by eggs in body cavity) with more prominent mid-lateral stripe, and less conspicuous dorsolateral stripe, otherwise with numerous melanophores, above and below mid-lateral stripe, from head to caudal-fin base. Middle of scale rows two and four above mid-lateral stripe with concentration of

Fig. 2. *Nanosphronemus gemma*, MTD 40216, female 16.4 mm (top) and putative male 16.2 mm SL (bottom), in lateral view, illustrating more prominent, darker pigmentation.

melanophores in the middle of scale, producing three narrow parallel stripes. Body below mid-lateral stripe with numerous melanophores, but less densely distributed. Melanophores also present along pectoral-fin rays, and dorsal- and anal-fin spines and rays, as well as caudal-fin rays. Pelvic fin with few small melanophores.

Putative male (no eggs in body cavity) with very dark colouration (Fig. 2). Mid-lateral stripe black, three scales wide, covering almost entire lateral and ventral area of body, leaving only ventral part of head and body less darkly pigmented. Mid-lateral stripe separated from dorsolateral stripe by lighter interstripe of ½ scale width. Dorsolateral stripe dark red-brown and black, not well separated from dark dorsal area of head and body, except in posterior half of caudal part of body. Dorsal- and anal-fin spines and rays dark brown to black; caudal-fin rays and intermittent membranes also densely covered with melanophores giving the fin a darker appearance than in females or formalin preserved specimens. Pectoral and pelvic fins with melanophores along margins of rays, but overall appearing translucent to whitish opaque.

Colouration in life. Putative females similar in colour pattern to formalin-preserved specimens, with prominent mid-lateral stripe, but with series of blue-green iridescent spots on each scale, and iridescence on postorbital area (Fig. 3a). Dorsolateral stripe not clearly demarcated from brown dorsal third of body, but black mid-lateral stripe and brown dorsal area separated by light cream interstripe. Dorsal- and anal-fin spines light brown, caudal, pectoral and pelvic fin translucent.

Putative males overall darker with more iridescent scales on mid-lateral stripe and area below it (Fig. 3b). Dorsolateral stripe red, dorsal and anal fins dark with iridescent margins. Sexually active males (Fig. 3c) with very dark, almost black lower two-thirds of body, and head covered in numerous blue-green iridescent spots from sub- and postorbital area to caudal peduncle. Dorsolateral stripe 1½ to 2 scales wide, a bright, neon red from behind eye to caudal peduncle. Dorsal most area of head and body black, separated from dorsolateral neon-red stripe by narrow lighter stripe. Dorsal, anal, and caudal fins black. Bases of dorsal and anal fins also with numerous specks of blue-green iridescence; both fins with iridescent margins. Pectoral fins hyaline except small melanophores lining margins of fin rays. Pelvic fins dusky to black.

Distribution. Unclear at present: reported from undisclosed area near Huế in Central Vietnam.

Etymology. The species name is derived from the Latin word for jewel, ‘gemma’, alluding to the stunning colouration of sexually mature males. A noun in apposition.

Remarks. Our aquarium observations show that during reproduction, male *Nanosphronemus* build a small bubble-nest underneath overhanging structures, such as plant leaves, in which they embed their eggs (Fig. 7). Nests are guarded by the male.

Osteology (Figs. 8–12)**.** Based on 16.2 mm SL male (MTD 40216). Skull bones mostly well-ossified (Figs. 8–9). Neurocranium with small narrow nasal, large wide frontal,

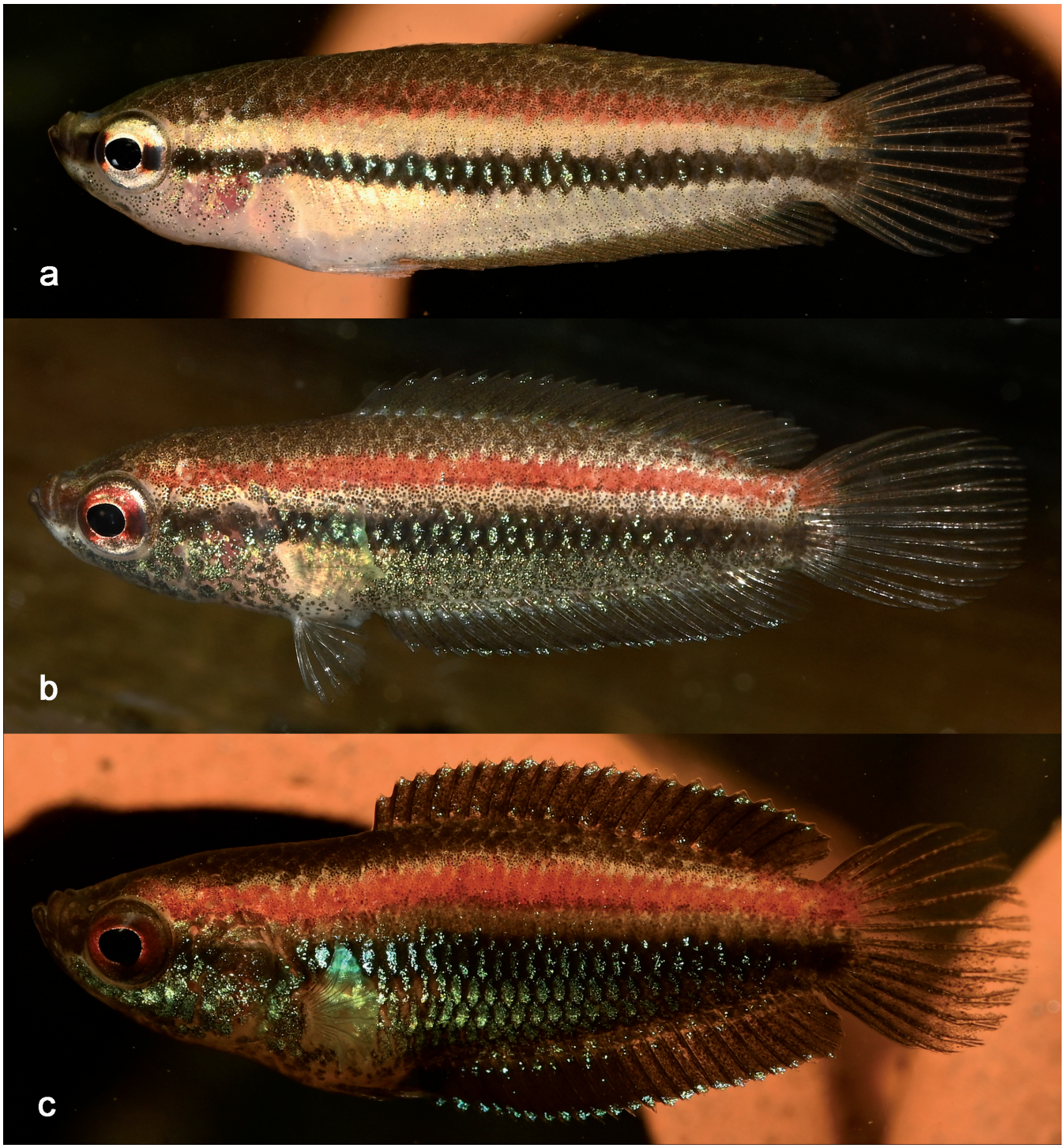

Fig. 3. *Nanosphronemus gemma*, live colouration, not preserved, all ca. 16 mm SL in lateral view. a, putative female above, note absence of red stripe in dorsal half; b, putative male in normal colouration, note presence of red stripe above and darker pigmentation below mid-lateral stripe; c, putative male in breeding colouration, note overall darker colouration of body and also fins, presence of bright red stripe and highly iridescent scales in mid-lateral stripe and below on head and body.

parietal and supraoccipital forming most of the neurocranial dorsal surface (Figs. 8, 9). Only frontal with lateral line canal along lateral margin (Fig. 9). Frontals meeting each other in irregular s-shaped suture. Posterior part of frontals separated by large supraoccipital in dorsal midline, also widely separating parietals. Supraoccipital with moderate crest above meeting point of exoccipitals (Fig. 9). Epiotic large with flat lateral process on dorsal surface to accommodate upper limb of forked posttemporal and with prominent posterior process to which epaxial musculature attaches. Pterotic short but well-developed, sutured to parietal and epiotic and forming posterior lateral margin of neurocranium (Fig. 9). Dorsal surface of pterotic with depression overlain by triangular extrascapular, which carries a lateral line canal. Lateral ethmoid forming large lateral wing at anterior margin of very large orbit (Fig. 9). Mesethmoid a dome shaped bone with deep median cavity to house very long ascending process of premaxilla, thus bulging into orbit in midline.

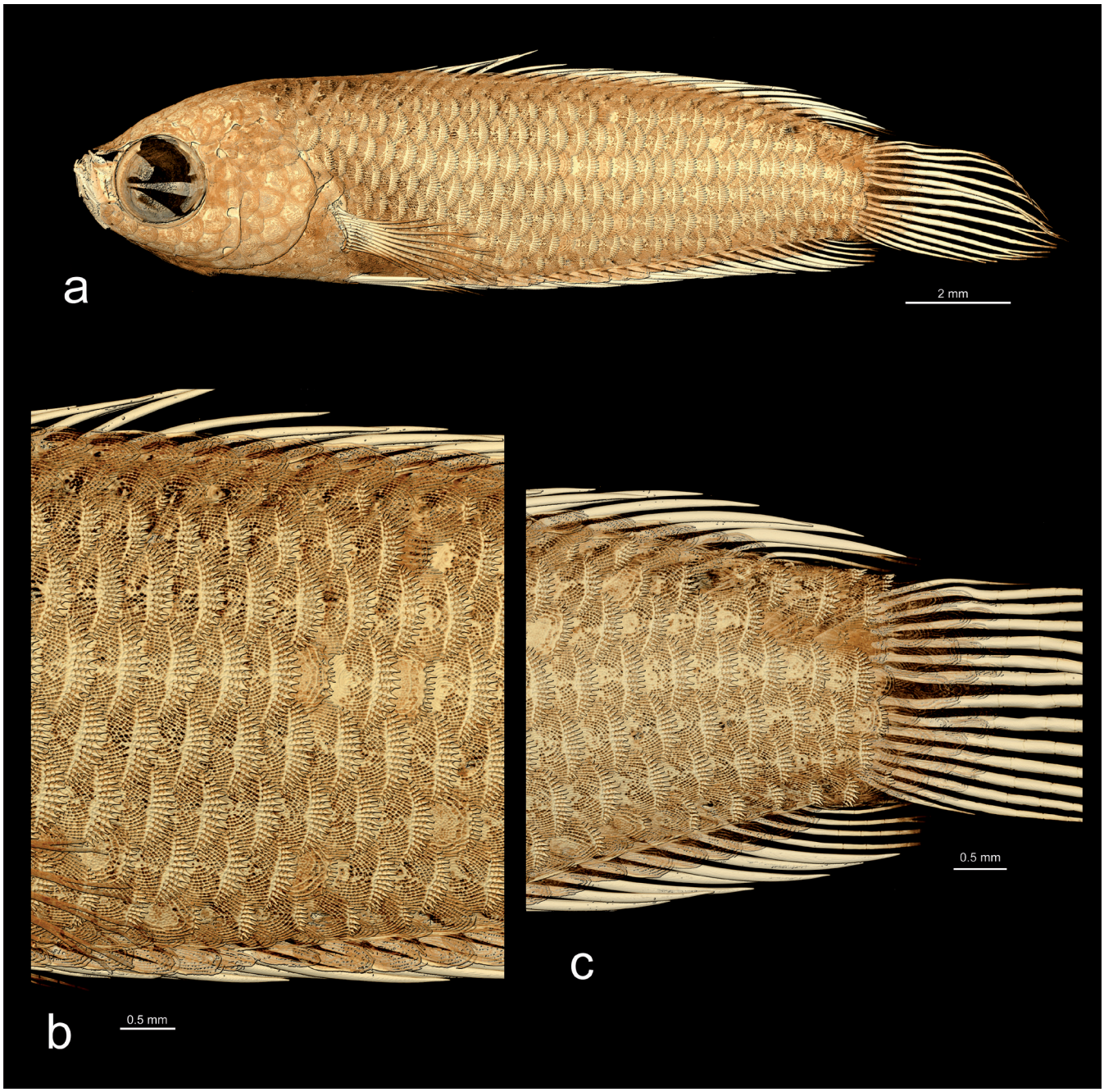

Fig. 4. *Nanosphronemus gemma*, MTD 40216, female, 16.4 mm SL, rendered CT-images of scalation in lateral view. a, entire body; b, posterior abdominal and anterior caudal region; c, posterior caudal region and caudal-fin base.

Pterosphenoid narrow, restricted to dorsoposterior margin of orbit (Fig. 9). Autosphenotic barely visible in dorsal view, but with prominent ventrally directed process on lateral face to which infraorbital ring is tightly bound anteriorly, with both forming posterior margin of orbit. Prootic large with orbital part housing trigemino-facial chamber and postorbital part forming cranial floor and anterior half of otic bulla. Basioccipital with short, paired pharyngeal processes to which upper pharyngeal jaws articulate and contributing posterior half of otic bulla and median articular facet of tripartite occipital condyle. Exoccipitals completely surrounding foramen magnum and contributing pair of dorsal articular facets of tripartite occipital condyle (Fig. 9c). Vomer with squarish anterior head and tapering posterior part reaching to level of anterior third of orbit and housed in median groove of parasphenoid (Fig. 9d). Parasphenoid overall narrow with slightly wider anterior part, tapering orbital section, wider ascending processes right at postorbital region and a prominent phraryngeal process at posterior end supporting four pharyngeal parasphenoid teeth (Fig. 9). In orbital area, parasphenoid with small anterodorsally directed process approaching posterior margin of orbitosphenoid (Fig. 9a).

Lachrymal and six additional infraorbitals surrounding large orbit anteriorly, ventrally and posteriorly as half ring of seven small ossicles (Figs. 8, 10a). Lachrymal largest with short lateral line canal at lateral face. Followed by flat but sequentially posteriorly wider infraorbitals 2–7. Uppermost caudal infraorbital (dermosphenotic) very tightly bound to anterior face of ventral process of autosphenotic. Sclerotic

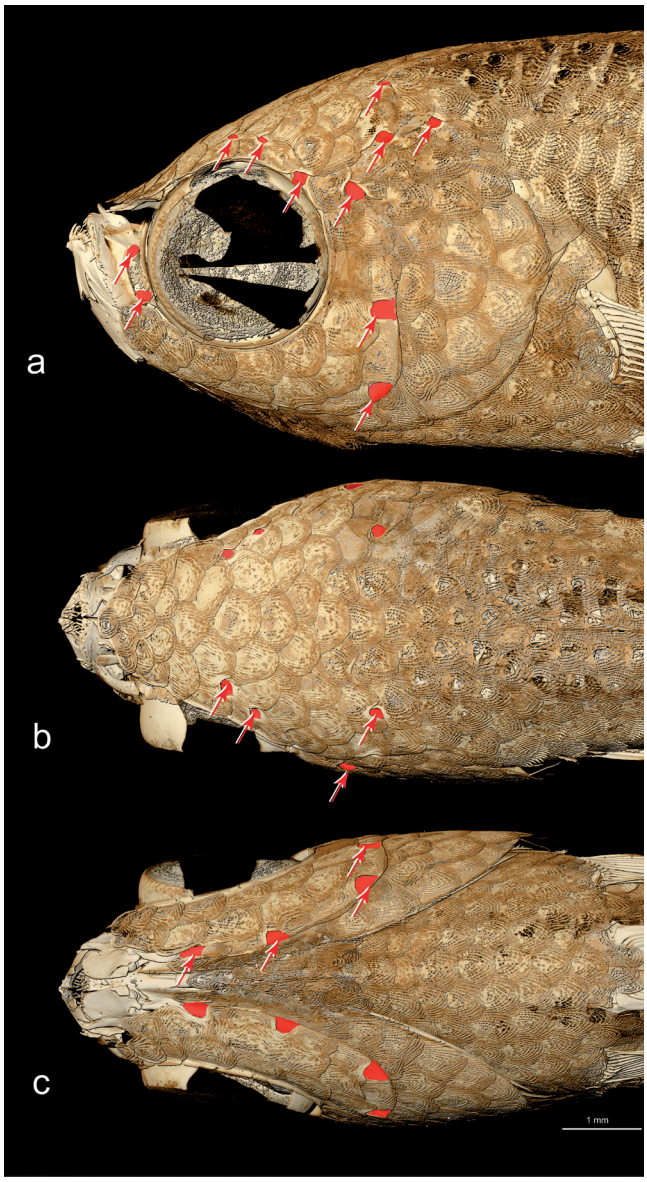

Fig. 5. *Nanosphronemus gemma*, MTD 40216, female, 16.4 mm SL, rendered CT-images of head scalation and lateral line canal pores in red and marked with arrows. a, in lateral view; b, in dorsal view; c, in ventral view.

bones large, well-ossified capping orbit anteriorly and posteriorly (Fig. 10b).

Hyopalatine arch and jaws (Fig. 10c, d). Opercular apparatus well-developed and with large opercle, preopercle, subopercle and interopercle. Preopercle with wide lateral-line canal. Hyomandibular with shallow anterior and posterior crests of membrane bone. Symplectic large with well-developed dorsal and ventral membrane bone crests. Dorsal crest in contact with posterior margin of endopterygoid. Quadrate with well-ossified articular condyle and long posteroventral process of membrane bone (Fig. 10c, d). Metapterygoid small and narrow, wedged in between symplectic and endopterygoid. Ectopterygoid absent. Palatine with compressed posterior part and tapering curved anterior process, articulating with lateral groove in maxilla. Maxilla short and stout with complex three-dimensional shape (Fig. 10c, d). Posterior section projecting posteroventrally beyond posterior tip

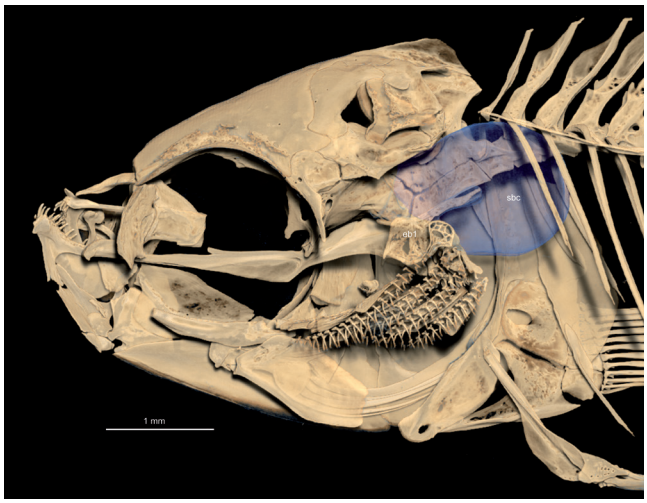

Fig. 6. *Nanosphronemus gemma*, MTD 40216, 16.2 mm SL. Rendered CT-image of suprabranchial chamber (sbc) and its association with epibranchial 1 (eb1) in lateral view. Left hyopalatine arch, infraorbitals and sclerotic bones digitally removed.

of premaxilla. Anterior section of maxilla with complex u-shaped articular groove on medial side housing proximal part of articular and long ascending process of premaxilla and additional articular groove laterally to accommodate long and curved process of palatine. Premaxilla short and stout with about a dozen curved conical teeth along anterior margin of articular process. Premaxilla also with very long ascending process, 1.5 times longer than articular process (Fig. 10c, d). Lower jaw short and compact. Small retroarticular capping posteroventral corner of lower jaw. Coronomeckelian an elongate ossicle in front of jaw articulation. Anguloarticular without lateral line canal but well-developed coronoid process and anteriorly directed process situated between large wing-like coronoid process of dentary and main body (Fig. 10c, d). Dentary with series of small conical teeth and patch of slightly more prominent teeth at symphysis.

Hyoid arch with short but well-ossified hypo- and ceratohyals (Fig. 11d, e). Anterior ceratohyal axe-shaped separated by straight cartilage-filled suture from posterior ceratohyal laterally, but on medial face sutured through long prongs, one posteriorly directed on anterior ceratohyal and one anteriorly directed from posterior ceratohyal. Only five branchiostegals rays, anterior articulating on medial side of anterior ceratohyal, posterior four on lateral side with 2–4 on anterior ceratohyal and 5 at suture between anterior and posterior ceratohyal (Fig. 11d, e). Urohyal a dorsoventrally orientated blade-like bone with anterodorsal cup-like articular facet (Fig. 11f, g).

Gill arches short and compact (Fig. 11a–c). Basihyal fused with basibranchial 1 forming an elongate compound element. Its posterior wider end underlying anterior half of short and wide basibranchial 2. Basibranchial 3 slightly more elongate with wider middle, fitting into space between hypobranchials 2 and 3. Hypobranchials compact, first more elongate, second widest, third with short ventrally directed processes. Ceratobranchials of similar length, ceratobranchial 1 widest with even wider distal third supporting large curved,

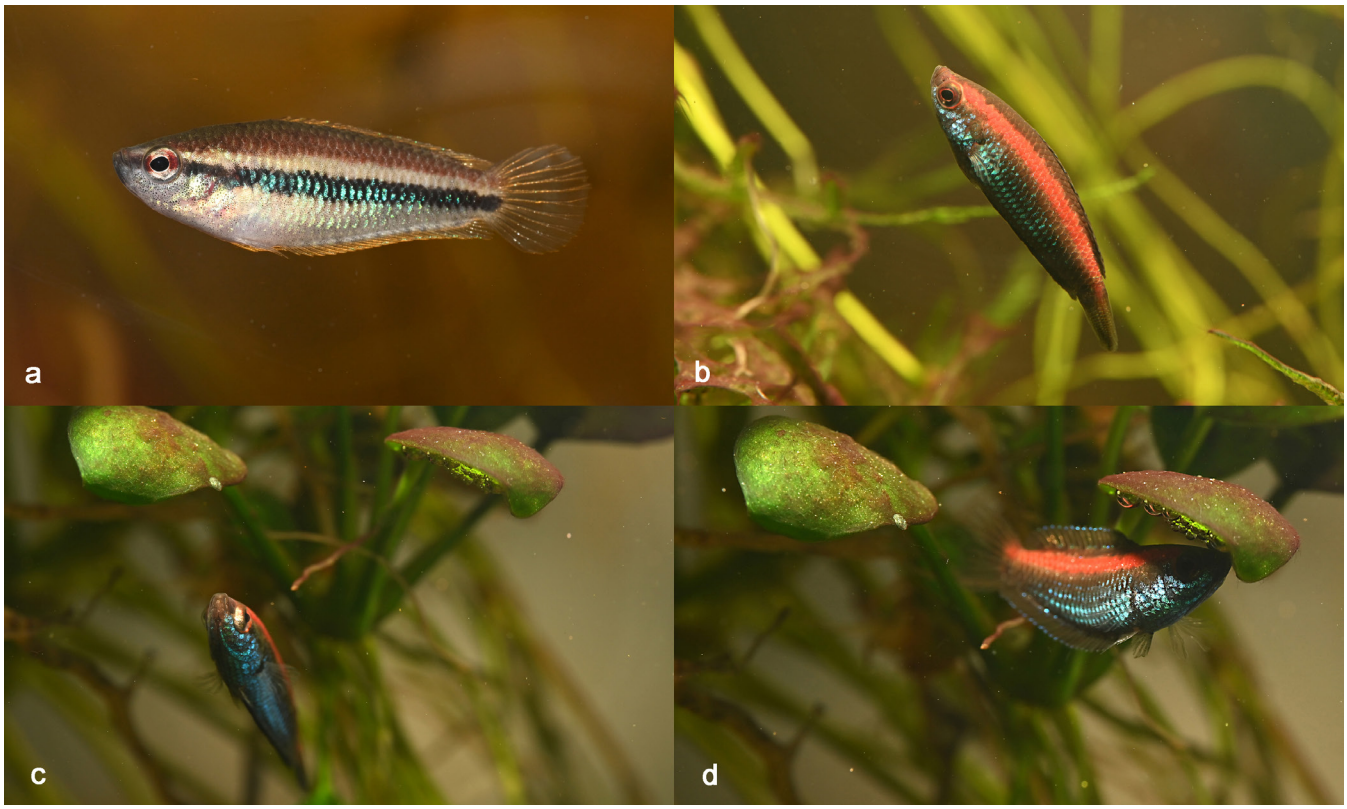

Fig. 7. *Nanosphronemus gemma*, not preserved, all ca. 18 mm SL. a, mature female with eggs; b, in breeding colouration and typical oblique courtship position, c, approaching bubble nest under plant leaf; d, adding air bubbles and embedding eggs into bubble nest.

modified gill raker guarding entrance to suprabranchial cavity. Elongate ceratobranchials 2–4 with small gill rakers along both margins in 2 and 3 and only anterior margin in ceratobranchial 4. Ceratobranchial 5 with large patch of teeth, teeth largest along posterior margin, smaller on rest of toothplate. Epibranchial 1 modified as labyrinth, its medially directed process articulating with prootic of otic capsule (Fig. 6). Complexly shaped labyrinthine plate composed of horizontal plate along stem of epibranchial and vertical antero-posteriorly directed plate. Epibranchials 2–4 elongate, closely set together, epibranchial 4 with wide articular head. Pharyngobranchial 2 with two narrow long processes and toothed ventral surface with about seven teeth. Pharyngobranchial 3 large, studded with large recurved teeth in its anterior and medial and smaller and shorter recurved teeth along its posterior and lateral face.

Shoulder girdle (Fig. 12) with long slender posttemporal, scale-like wide supracleithrum, large cleithrum and two postcleithra. Posttemporal with long upper and shorter lower limb. Supracleithrum wide but thin, with round articular head to accommodate ventral end of posttemporal. Postcleithrum 1 large and wide covering cleithrum and posterior part of scapula. Postcleithrum 2 shorter with pointed needle-like posteroventrally directed tip. Cleithrum supporting large scapula and upper anterior tip of coracoid on medial face and anteroventral process of coracoid on lateral face. Scapula with large foramen close to its anterior margin. Four pectoral radials, three upper radials articulating with posterior margin of scapula, largest fourth radial with posterior margin of coracoid. Basipterygium elongate with anteroventral flange of membrane bone. Basipterygium directed anterodorsally, articulating with medial face of large ventral cleithral flange.

Basipterygium of pelvic girdle articulating on medial side of cleithrum via long process with round cross-section (Fig. 12). Flange of membrane bone originating along lateral margin of main body of basipterygium and curving anteromedially. One spine and five rays articulating with lateral face of basipterygium.

Vertebrae with long neural spines, abdominal vertebrae 2–9 with anterior membrane bone flanges on neural spines (Fig. 8). Neural arch and spine of first vertebra autogenous, much more slender than subsequent arches and spines, sitting spatially removed above centrum 1 (Fig. 8b). Abdominal vertebrae 4–9 and first caudal vertebra with shorter (vertebrae 4–5) or longer (vertebrae 6–10) prezygapophyses. Parapophyses on anterior 5 vertebrae with horizontal orientation, on vertebrae 6–9 sequentially more ventrally directed. Series of 8 abdominal ribs, starting on vertebra 2, articulating with parapophyses and continued posteriorly into caudal region with additional ribs. First caudal vertebra with prominent haemal spine and lateral extensions of haemal arches (Fig. 8). Lateral extensions becoming sequentially shorter and less prominent, extensions absent from preural vertebrae 2 and 3. Series of nine caudal ribs supporting posteriorly elongated swimbladder extensions articulated with lateral extensions on caudal vertebrae 1–9 (Fig. 8c). Haemal arches of vertebrae 5–13 with anteroventrally directed pointed, spine-like processes, asymmetrically developed on either right or left haemal arch (Fig. 8c). Length of haemal arches

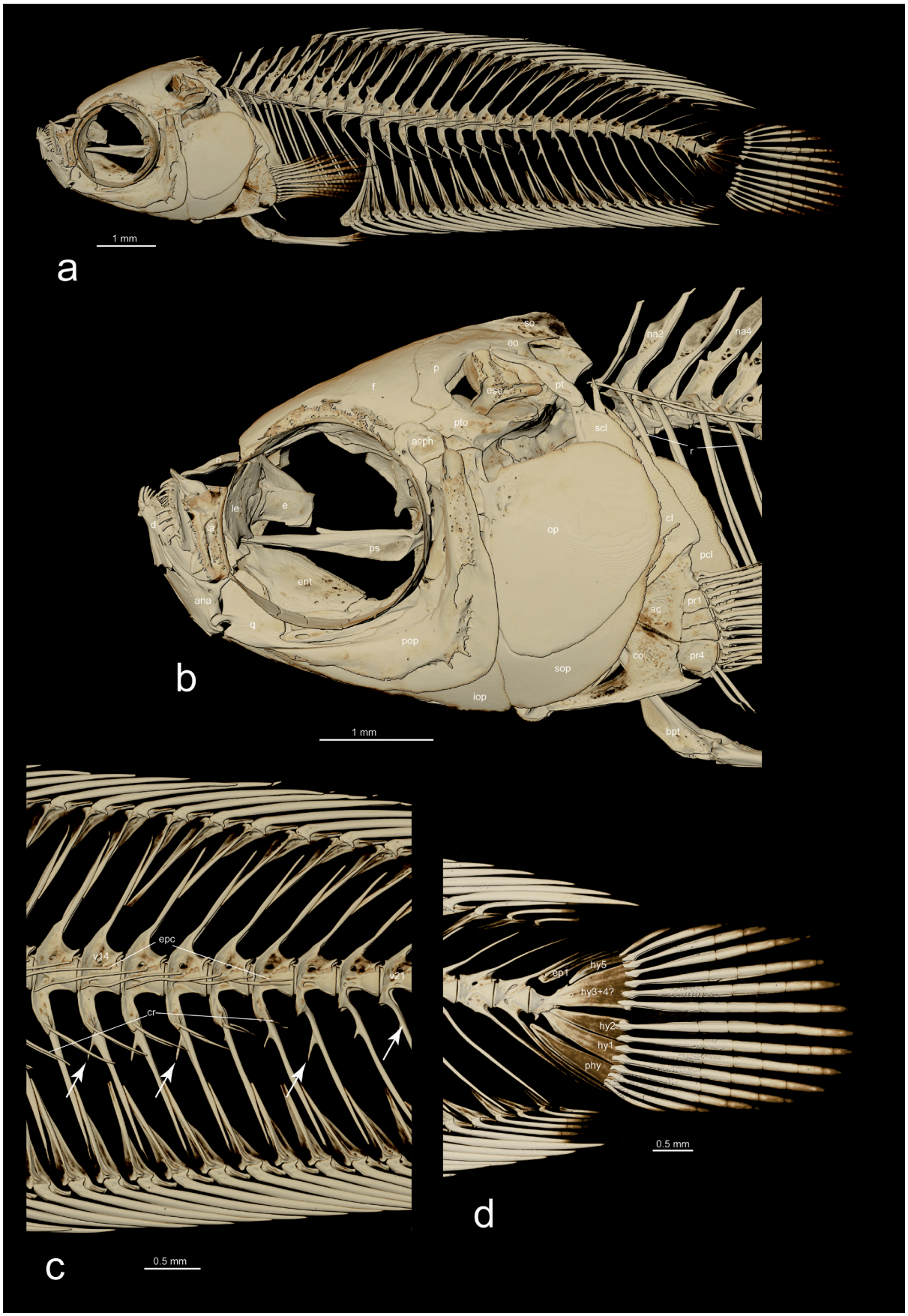

Fig. 8. *Nanosphronemus gemma*, MTD 40216, 16.2 mm SL. Rendered CT-images of skeleton in lateral view. a, entire body; b, head, shoulder girdle and anterior vertebrae; c, anterior caudal area, white arrows mark anterior processes on haemal arches; d, preural region and caudal fin. Abbreviations: ana, anguloarticular; asph, autosphenotic; cl, cleithrum; co; coracoid; cr, caudal ribs; d, dentary; e, ethmoid; eo, epiotic; ep, epural; epc, epicentrals; ent, endopterygoid; esc, extrascapular; f, frontal; hy, hypural; iop, interopercle; le, lateral ethmoid; n, nasal; na, neural arch; op, opercle; p, parietal; pcl, postcleithrum; phy, parhypural; pop, preopercle; pt, posttemporal; pto, pterotic; pr, pectoral radial; ps, parasphenoid; q, quadrate; so, supraoccipital; r, rib; sc, scapula; scl, supracleithrum; sop, subopercle; v, vertebra.

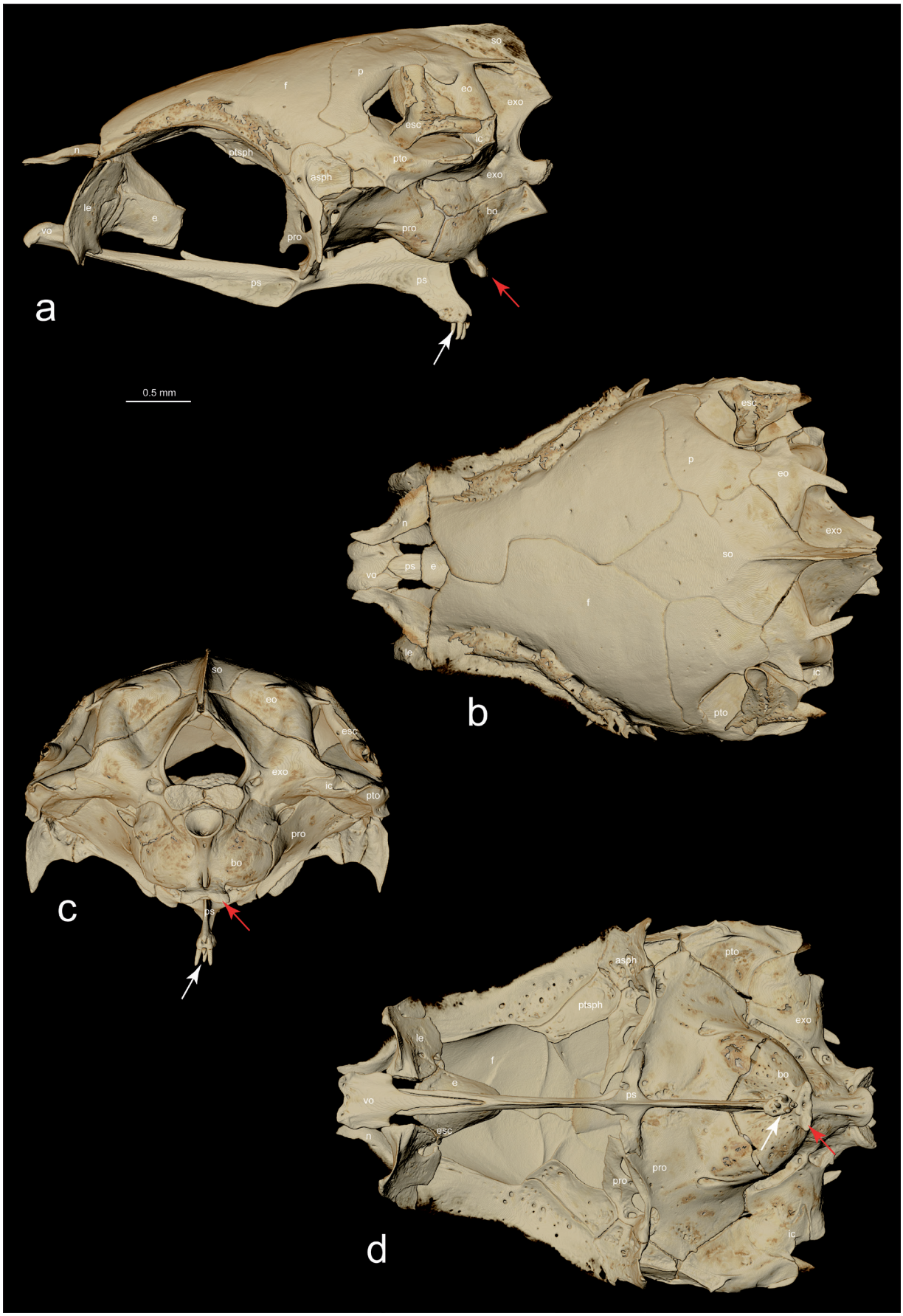

Fig. 9. *Nanosphronemus gemma*, MTD 40216, 16.2 mm SL. Rendered CT-images of neurocranium. a, lateral view; b, dorsal view; c, posterior view; d, ventral view. White arrow points to toothed pharnygeal process of parasphenoid, red arrow to pharyngeal process of basioccipital. Abbreviations: ana, anguloarticular; asph, autosphenotic; bo, basioccipital; d, dentary; e, ethmoid; eo, epiotic; esc, extrascapular; exo, exoccipital; f, frontal; le, lateral ethmoid; n, nasal; p, parietal; pto, pterotic; pr, pectoral radial; pro, prootic; ps, parasphenoid; so, supraoccipital, vo, vomer.

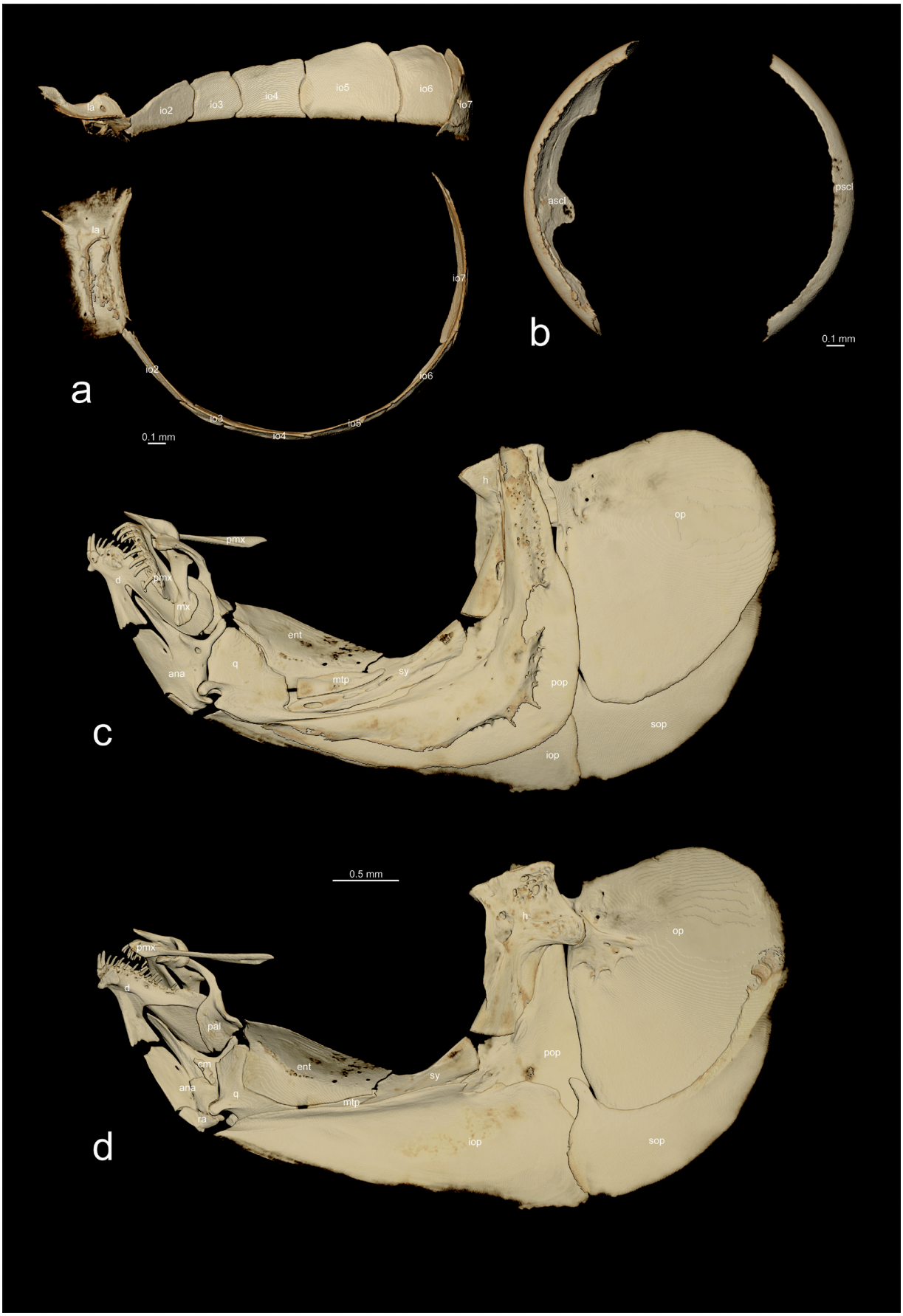

Fig. 10. *Nanosphronemus gemma*, MTD 40216, 16.2 mm SL. Rendered CT-images of infraorbital series, sclerotics, and hyopalatine arch. a, lachrymal and infraorbital bones in dorsal (above) and lateral views; b, sclerotic bones in lateral view; c, hyopalatine arch in lateral view; d, hyopalatine arch in medial view. Abbreviations: ana, anguloarticular; ascl, anterior sclerotic; cm, coronomeckelian; d, dentary; e, ethmoid; eo, epiotic; ep, epural; ent, endopterygoid; io, infraorbital; iop, interopercle; la, lachrymal; mtp, metapterygoid; mx, maxilla; op, opercle; pal, palatine; pmx, premaxilla; pop, preopercle; pscl, posterior sclerotic; q, quadrate; ra, retroarticular; sop, subopercle; sy, symplectic.

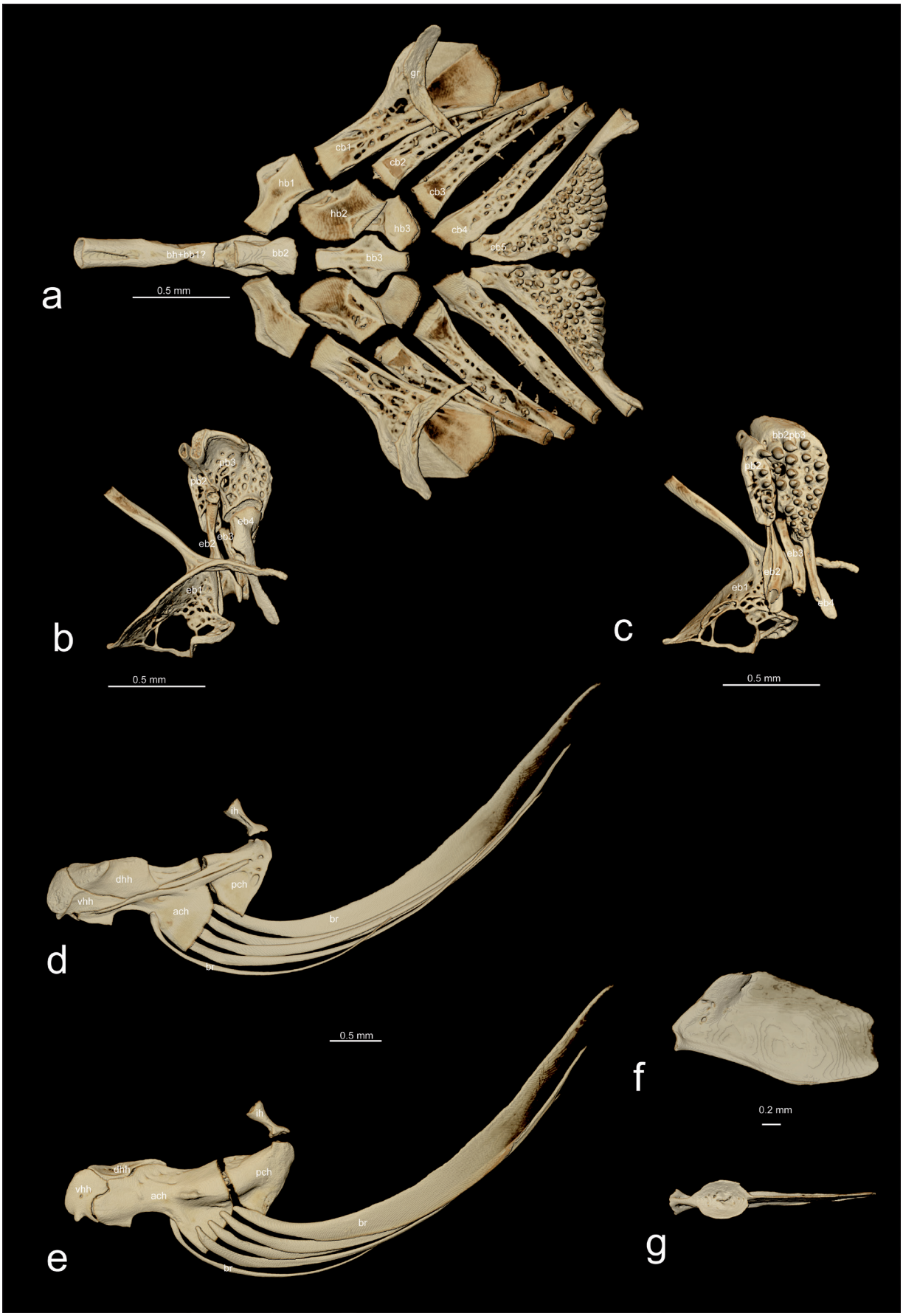

Fig. 11. *Nanosphronemus gemma*, MTD 40216, 16.2 mm SL. Rendered CT-images of ventral gill arches, hyoid bar and urohyal. a, ventral gill arches in dorsal view; b, dorsal gill arches in dorsal view; c, dorsal gill arches in ventral view; d, hyoid bar in lateral view; e, hyoid bar in medial view; f, urohyal in lateral view. g; urohyal in dorsal view. Abbreviations: ach, anterior ceratohyal; bb, basibranchial; bh, basihyal; br, branchiostegal ray; cb, ceratobranchial; dhh, dorsal hypohyal; eb, epibranchial; gr, greatly enlarged gill raker guarding entrance to suprabranchial cavity; hb, hypobranchial; ih, interhyal; pb, pharyngobranchial; pch, posterior ceratohyal; vhh, ventral hypohyal.

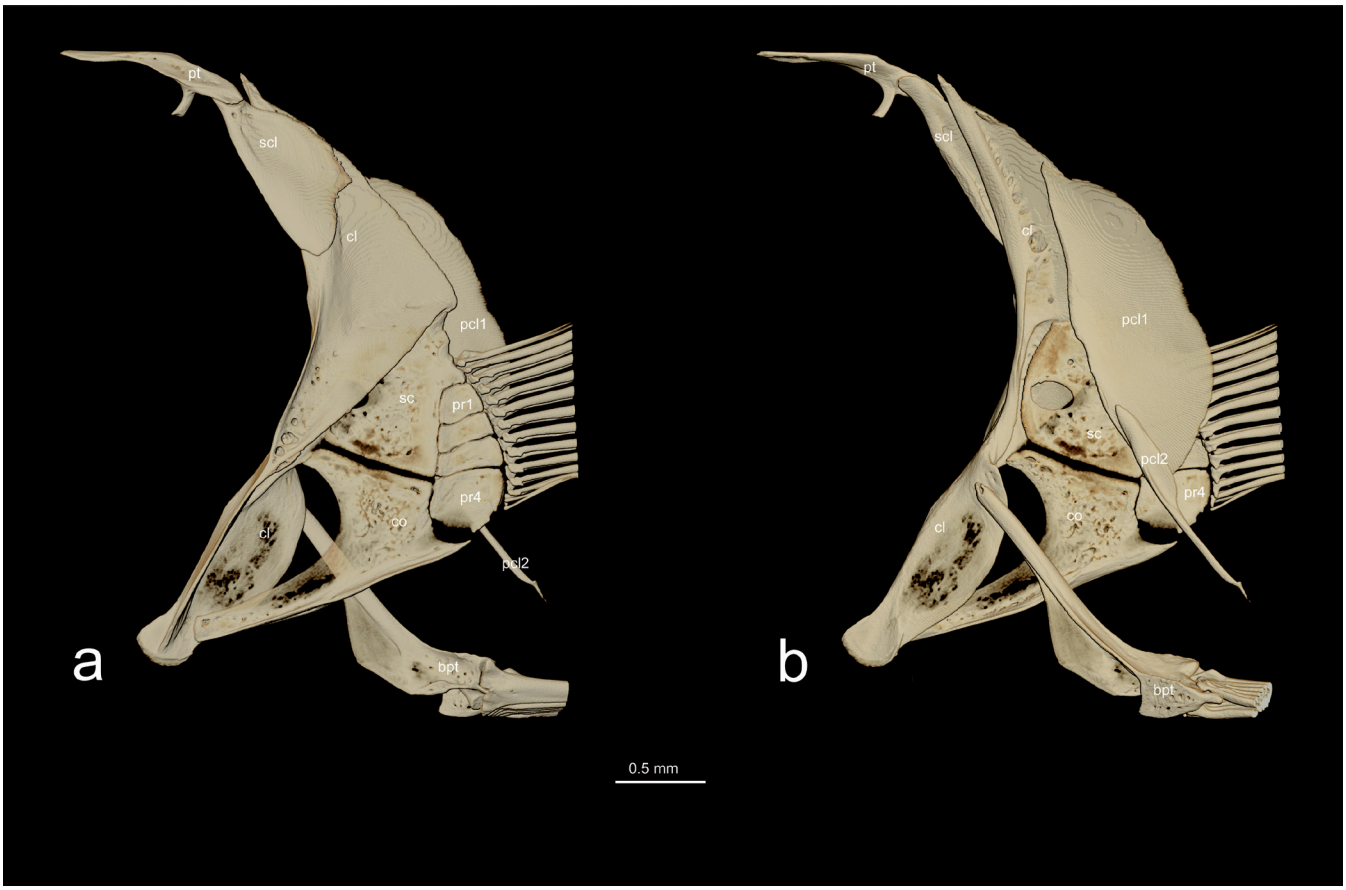

Fig. 12. *Nanosphronemus gemma*, MTD 40216, 16.2 mm SL. Rendered CT-images of shoulder girdle. a, lateral view; b, medial view. Abbreviations: bpt, basipterygium; cl, cleithrum; co; coracoid; pcl, postcleithrum; pt, posttemporal; pto, pterotic; pr, pectoral radial; sc, scapula; scl, supracleithrum.

plus spine greater than neural arches plus spine on the same vertebra with difference becoming more pronounced in posterior caudal vertebrae.

Abdominal vertebrae and anterior eight caudal vertebrae with epicentral intermuscular bones (Fig. 8a–c), articulating on neural arch of first vertebra, on articular heads of ribs on vertebrae 2–9, on haemal arches on vertebrae 10–15 (caudal vertebrae 1–6) and on centra on vertebrae 16–17 (caudal vertebrae 7–8).

Caudal fin with autogenous parhypual and two hypural plates (hypural 1 and 2) in ventral half and two hypural plates (fused hypurals 3 and 4? and hypural 5) in dorsal half (Fig. 8d). Hypurals 1 and 2 articulating with ural centrum, upper hypural plate (fused hypurals 3 and 4?) fused to ural centrum and hypural 5 situated along dorsal margin of upper hypural plate slightly removed from distalmost tip of ural centrum. One epural wedged in between neural spine of preural centrum 2 and hypural 5.

Dorsal fin with 21 spines and 2 rays (Fig. 8a). Serially associated pterygiophores inserted between neural spines 4 and 5 posteriorly to neural spines 24 and 25, mostly in 1/1 pattern (1 spine, 1 pterygiophore, 1 spine etc.), except both pterygiophores 10 and 11 situated between neural spines 14 and 15. Anal fin with 22 spines and 5 rays, with 4 spines articulated in front of first haemal spine.

Table 2. Meristic information for holotype (ZRC 70244, in parentheses behind ranges) and nine paratypes (ZRC 70070) of *Nanosphronemus gemma*.

Dorsal-fin rays	XIX–XXI+2–3 (XXI+3)
Anal-fin rays	XXI–XXIV+4–5 (XXIII+5)
Caudal-fin rays	1+6+6+2 (1+6+6+2)
Pectoral-fin rays	10–11 (11)
Pelvic-fin rays	I+5 (I+5)
Lateral scales	28–29 (29)
Vertebrae	8–9+19–20=28–29 (9+20=29)

Anteriormost anal-fin pterygiophore wider than subsequent pterygiophores, supporting two rays, one in supernumerary and one in serially associated position. Two additional pterygiophores situated behind wide first anal pterygiophore and in front of first haemal spine. Anal-fin pterygiophores of caudal region arranged with haemal spines in pattern of 1/2/1/2/1/1/1/2/1/2/1/1/2/2/2.

Molecular results. Newly generated nucleotide sequences of *Nanosphronemus* were deposited in GenBank under accession numbers PZ713666 and PZ714198–PZ714200. The final alignment length used for the phylogenetic analyses

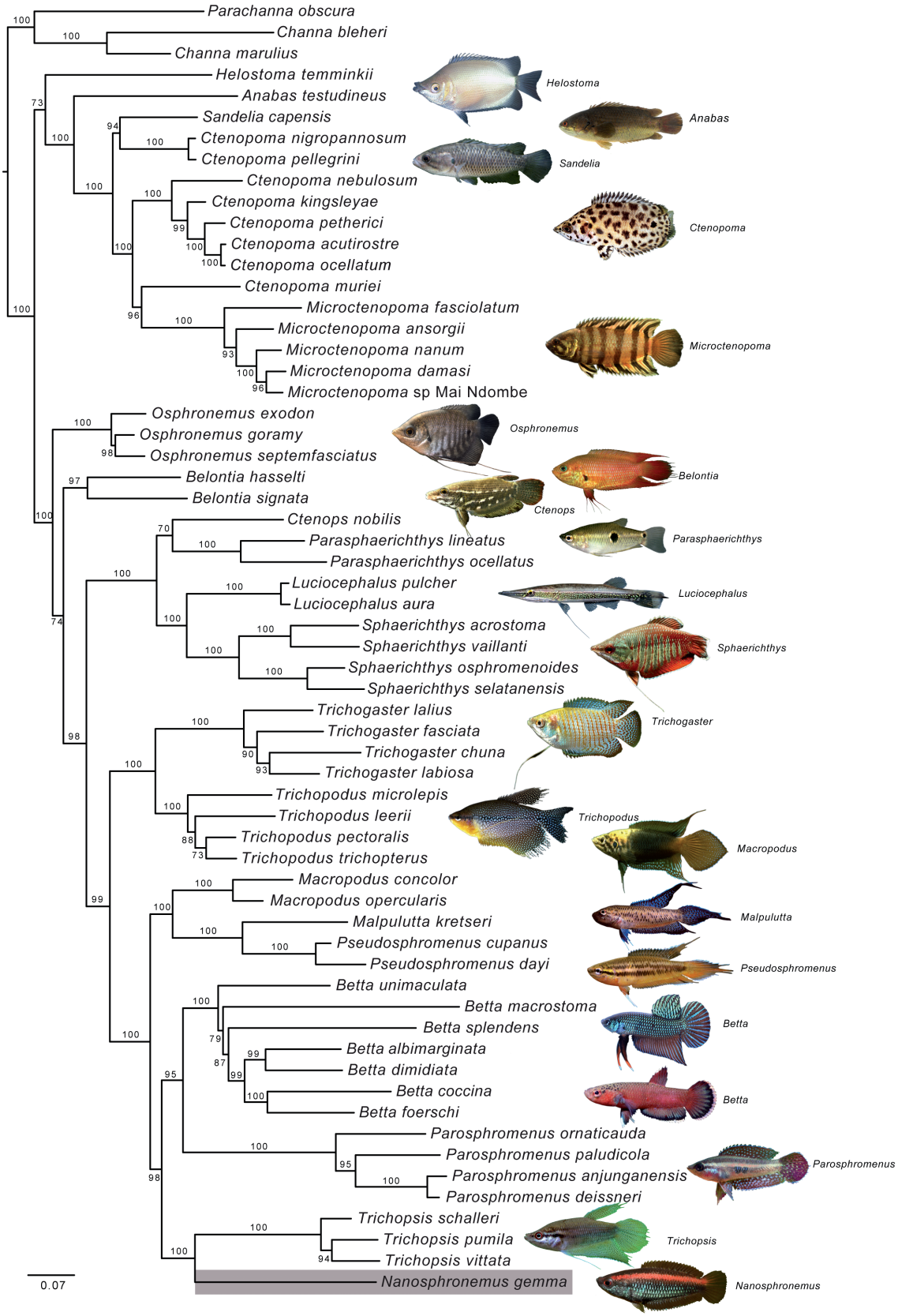

Fig. 13. Rooted phylogram of the maximum likelihood analysis (-ln L = -58148.3058) of the combined mitochondrial and nuclear data set for labyrinth fishes. *Nanosphronemus gemma* (highlighted in grey) is recovered as sister group of *Trichopsis*. Bootstrap values are show above or below branches. Photos with credit from top to bottom: *Helostoma temminkii* (Till Luckenbach), *Anabas testudineus* (Heok Hui Tan), *Sandelia capensis* (Frank Schäfer), *Ctenopoma acutirostre* (Jürgen Schmidt), *Microctenopoma ansorgii* (Horst Linke), *Osphronemus goramy* (Frank Schäfer), *Belontia signata* (Hiranya Sudasinghe), *Ctenops nobilis* (Horst Linke), *Parasphaerichthys ocellatus* (Till Luckenbach), *Luciocephalus aura* (Heok Hui Tan), *Sphaerichthys vaillanti* (Zhou Hang), *Trichogaster lalia* (Horst Linke), *Trichopodus leerii* (Horst Linke), *Macropodus ocellatus* (Horst Linke), *Malpulutta kretseri* (Jürgen Schmidt), *Pseudosphromenus dayi* (Frank Schäfer), *Betta smaragdina* (Horst Linke), *Betta channoides* (Zhou Hang), *Parosphromenus linkei* (Zhou Hang), *Trichopsis vittata* (Frank Schäfer), *Nanosphronemus gemma* (Ralf Britz).

was 4,275 base pairs (bp) (cytb 1,137 bp; 12S rRNA, tRNA Val, 16S rRNA 1,659 bp; RAG1 1,479 bp). A total of 2,557 COI sequences were downloaded from Genbank (n=1,757) and BOLD (n=800), and the final alignment length used for the calculation of genetic distances, including the newly determined *Nanosphronemus* COI sequence, was 630 base pairs.

The result of the ML analysis based on the combined mitochondrial and nuclear data set is shown in Fig. 13. The topology of the phylogenetic tree is in full agreement with previous results regarding phylogenetic interrelationships of anabantoid genera (Rüber et al., 2006). Our analysis recovered *Nanosphronemus* as the sister group of *Trichopsis* with a bootstrap support of 100.

Minimum uncorrected p-distances in the COI barcoding gene between *Nanosphronemus* and all other labyrinth fish genera ranged from 10.6–23.5%. The range of uncorrected p-distances between *Nanosphronemus* and its closest sister group *Trichopsis* was 20.0–22.6 % (n=273), and 10.6–27.6 % (n=1108) and 19.0–21.4% (n=135) to the closely related genera *Betta* and *Parosphromenus* respectively.

DISCUSSION

With their roughly 170 species, the Anabantoidei show quite a range in sizes from the smallest, such as *Parosphromenus ornaticauda* at 19.4 mm SL (Kottelat, 1991) and *Parasphaerichthys lineatus* (Britz & Kottelat, 2002) at 18.7 mm SL, to the giant gouramis of the genus *Osphronemus* with lengths up to at least 550 mm SL (Roberts, 1992). Along with *Parasphaerichthys lineatus*, *Nanosphronemus gemma* with the same maximum size of 18.7 mm SL, is currently the smallest anabantoid.

In addition to its size and the colour pattern of mature males with their neon-red dorsolateral stripe, *Nanosphronemus gemma* can be readily distinguished from any other anabantoid by its unique dorsal- and anal-fin ray count with XIX–XXI+2–3 dorsal- and XX–XXIV+4–5 anal-fin rays. The only other anabantoid taxon that approaches this high number of dorsal- and anal-fin spines is *Macropodus ocellatus* (Table 3). Rarely, individuals of *M. ocellatus* have XIX dorsal-fin spines; however, the number of dorsal-fin rays is higher and ranges from 5–9 rays (Freyhof & Herder, 2002), while *N. gemma* has only 2–3 dorsal rays. The same is true for the anal fin, in which the number of spines ranges from 16–22 in *Macropodus ocellatus*, and 17–21 in *M. opercularis*, *M. spechti*, and *M. erythropterus* (Freyhof & Herder, 2002), thus reaching into the range of the number of anal-fin spines in *Nanosphronemus.* The four species of *Macropodus* and the latter differ by the number of soft rays with 7–12 in *M. ocellatus*, 11–14 in *M. opercularis* and *M. spechti*, and 13–17 in *M. erythropterus* (Herder & Freyhof, 2002), but only 4–5 in *N. gemma*.

Nanosphronemus has a number of morphological characters that are unusual or unique among anabantoids. The very long ascending processes of the premaxillae are housed in a dome-like ethmoid in *Nanosphronemus*, which protrudes into the orbit but does not contact the parasphenoid. Usually in anabantoid taxa with long ascending processes, these slide along the flattened dorsal surface of the ethmoid, as e.g., in *Luciocephalus* (Liem, 1967a). The only anabantoids in which ascending processes are housed in a similar protruding dome-like ethmoid are species of the genus *Trichogaster* (Liem, 1963, fig. 25 for *T. lalia*; Liem, 1961, pl. 39 for *T. fasciata*). We note here that the same image illustrating *T. fasciata* in Liem (1961, pl. 39) is incorrectly labelled *Trichopodus trichopterus* in Liem (1963, fig. 37).

Nanosphronemus has only five branchiostegal rays, a character state it shares with all members of the Luciocephalinae and Trichogastrinae, while all other anabantoids have the full complement of six branchiostegals (Britz, 2001). This was one of the putative synapomorphies used by Britz (2001) to support monophyly of the genera *Luciocephalus*, *Ctenops*, *Sphaerichthys*, *Parasphaerichthys*, *Trichogaster*, and *Trichopodus*. This hypothesis, however, did not gain support from molecular data, in which the first four genera, as Luciocephalinae, and the last two as Trichogastrinae, were recovered as successive clades with the Trichogastrinae as the sister group to the Macropodusinae, and not Luciocephalinae (Rüber et al., 2006).

Another derived character with phylogenetic significance used by Britz (2001) is the origin of Baudelot's ligament. Primitively, it inserts on the lateral face of the basioccipital between the cranial articulation with the first vertebra and its pharyngeal process. In Luciocephalinae and Trichogastrinae, Baudelot's ligament inserts on a posteriorly directed median process of the basioccipital, which reaches posteriorly at least beyond the articulation of the first and second centrum (Britz, 2001). The only exception is the genus *Parasphaerichthys*, in which Baudelot's ligament inserts on the first neural arch. In all Macropodusinae, Baudelot's ligament inserts on the neural arch of the second vertebra (Britz, 2001). Interestingly, *Nanosphronemus* shows again a different autapomorphic condition, in which Baudelot's ligament inserts on the exoccipital close to the base of the margin of the foramen magnum.

Nanosphronemus shows additional unusual characters. The lateral line canals of the nasal and pterotic, as well as those of the anguloarticular and dentary, are absent in *Nanosphronemus* but present in other anabantoid genera (Liem, 1963). This reduction of the cranial lateral-line system seems unique among anabantoids, but other tiny taxa not covered by Liem (1963) would need to be checked for this character. *Nanosphronemus* is also unusual among anabantoids in having the anteriormost rib articulating on the second vertebra. Liem (1963) cited the anabantoid taxa *Helostoma*, *Belontia*, and *Sphaerichthys* as having a rib on the second vertebra and *Trichogaster* as having ribs on all abdominal vertebrae. This, however, is contradicted by Hyrtl (1863) for *B. hasselti* and by Britz (2001) for *Belontia signata* and *Sphaerichthys,* as well as our radiographs of these taxa and *Helostoma* and *Trichogaster* (see Table 3).

Table 3. Comparison of vertebral, dorsal- and anal-fin ray counts in *Nanosphronemus gemma* (ZRC 70244, 70070; MTD 40216) with those of members of other anabantoid genera. Numbers in parentheses behind a count indicate the number of specimens with that count. The abbreviation ifHS refers to number of anal fin spines articulating with pterygiophores situated in front of 1st haemal spine.

	Vertebrae	**D-spine**	**D-soft**	**A-spine**	**A-soft**
Nanosphronemus gemma ZRC 70244, 70070	9+19(5), 9+20(9) 8+20(1)	19(1), 20(4), 21(10)	2(1), 3(14)	21(1), 22(6), 23(7), 24(1), 4 ifHS (14), 3 ifHS(1)	4(7), 5(8)
N. gemma MTD 40216	9+19(2)	20(2)	2(1), 3(1)	21, 4 ifHS(1) 22, 4 ifHS(1)	4(1), 5(1)
Anabantidae					
Ctenopoma kingsleyae ZRC 67921	10+16	17	10	9, 1 ifHS	11
Microctenopoma ansorgii ZRC uncatalogued	9+17	19	6	11, 2 ifHS	8
M. fasciolatum ZRC 51466	9+17	16	9	10, 3 ifHS	10
Anabas testudineus ZRC 15201	10+15	17	9	10, 3 ifHS	10
Helostomatidae					
Helostoma temminckii ZRC 46213	15+15	18	14	14, 11 ifHS	17
Osphronemidae					
Osphroneminae					
Osphronemus gouramy ZRC 42927	11+20	13	12	10,7 if HS	20
Belontiinae					
Belontia hasselti ZRC 32476	11+17	17	12	15, 6 ifHS	12
Luciocephalinae					
Ctenops nobilis ZRC 51700	10+19	5	8	4, 4 ifHS	27
Parasphaerichthys ocellatus ZRC 46189	9+16	4	5	13, 4 ifHS	11
Sphaerichthys osphromenoides ZRC 39966	9+17	10	9	7, 4 ifHS	22
Luciocephalus pulcher ZRC 69751	19+21	2	8	2, 2 ifHS	16
Trichogastrinae					
Trichopodus pectoralis ZRC 32202	10+22	6	10	10, 6 ifHS	37
Trichogaster fasciata ZRC 54872	10+18	16	12	17, 6 ifHS	17
Tr. lalia ZRC 38908	10+17	16	8	17, 6 iFHS	15
Macropodusinae					
Macropodus opercularis ZRC 64411	9+19	16	6	21, 5 ifHS	12
Pseudosphromenus cupanus ZRC 63249	9+19	15	6	19, 5 ifHS	12
Malpulutta kretseri ZRC 51690	9+19	9	5	16, 4 ifHS	10
Betta bellica ZRC 51469	10+24	2	9	2, 2 ifHS	30
B. pugnax ZRC 46736	10+19	1	8	2, 2 ifHS	24
B. burdigala ZRC 70027	9+21	1	13	1, 0 ifHS	24
B. uberis ZRC 53102	9+20	1	14	2, 0 ifHS	24
Parosphromenus allani ZRC 61241	9+19	12	6	13, 3 ifHS	8
P. parvulus ZRC 65525	9+18 (2)	10 (2)	4(1), 5(1)	9, 3 ifHS (2)	10(2)
P. paludicola ZRC 42143	9+20	17	5	14, 3 ifHS	14
Trichopsis vittata ZRC 42980	9+20	4	8	8, 5 ifHS	26

We suspect that Liem (1963) overlooked the first vertebra, which is tightly wedged in between the occiput and second vertebra, and has an autogenous neural arch.

Our molecular data also suggest that *Nanosphronemus* represents a separate genus among osphronemid anabantoids. Our analysis recovered it as the sister group to the genus *Trichopsis*, the croaking gouramis. While this result is based on comprehensive taxon sampling, this hypothesis should be further tested with larger scale molecular markers and eventually genome level analyses.

Nanosphronemus can be readily distinguished from *Trichopsis* by its much longer dorsal fin with XIX–XXI+2–3 dorsal-fin rays, while *Trichopsis* (Table 3) has a short dorsal fin with fewer spines (IV), but more rays (8). There is almost no difference in the total number of anal-fin rays, the ratio of spines to soft rays is very different: *Nanosphronemus* has XX–XXIV+4–5 anal-fin rays, while *Trichopsis* has VIII+26. In addition, the skeletal modifications we found in *Nanosphronemus*, are all absent in *Trichopsis*.

Despite the monographic morphological treatment of anabantoids by Liem (1963), we feel that many anatomical characters require re-assessment, which will be the prerequisite for a comprehensive morphology-based phylogenetic hypothesis. With the power and detail possible today using high quality µ-CT scanning, as in our case of *Nanosphronemus*, such a study would be a worthwhile project that would lead to a better understanding of the morphological changes that accompanied the evolution of this interesting group of teleosts.

ACKNOWLEDGEMENTS

We are grateful to Herbert Nigl, Aquarium Dietzenbach, who provided specimens for live photography and CT scanning. Amanda Pinion, Senckenberg Dresden, helped us with her unparalleled expertise in µ-CT scanning and subsequent data processing to generate the rendered images. The µCT scans of *Nanosphronemus gemma* were obtained with a Zeiss Context, which was acquired through the financial support of the European Regional Development Fund (EFRE) and processed and imaged with software acquired through a grant from the Sächsisches Staatsministerium für Wissenschaft, Kultur und Tourismus (SMWK) through their TG-70 funding stream. THH acknowledges funding and resources from LKCNHM and NUS; Wei-Cheng Jhuang, Jonathan Poh, and Lê Trung Hiêu, for specimens. Rohan Pethiyagoda, Rajeev Raghavan and one anonymous reviewer provided helpful comments.

LITERATURE CITED

Bader R (1937) Bau, Entwicklung und Funktion des akzessorischen Atmungsorganes der Labyrinthfische. Zeitschrift für Wissenschaftliche Zoologie, 149: 323–401. https://doi.org/10.1007/BF00304447

Britz R (1994) Ontogenetic features of *Luciocephalus* (Perciformes, Anabantoidei), with a revised hypothesis of anabantoid intrarelationships. Zoological Journal of the Linnean Society, 112: 491–508. https://doi.org/10.1006/zjls.1994.1055

Britz R (2001) The genus *Betta* — monophyly and intrarelationships, with remarks on the subfamilies Macropodinae and Luciocephalinae. Ichthyological Exploration of Freshwaters, 12: 305–318.

Britz R & Cambray J (2001) Structure of egg surfaces and attachment organs in anabantoids. Ichthyological Exploration of Freshwaters, 12: 267–288.

Britz R & Kottelat M (2002) *Parasphaerichthys lineatus*, a new species of labyrinth fish from southern Myanmar (Teleostei: Osphronemidae). Ichthyological Exploration of Freshwaters, 13: 243–250.

Britz R, Kokoscha M & Riehl R (1995) The anabantoid genera *Ctenops*, *Luciocephalus*, *Parasphaerichthys* and *Sphaerichthys* as a monophyletic group: evidence from egg surface structure and reproductive behaviour. Japanese Journal of Ichthyology, 42: 71–79. https://doi.org/10.11369/jji1950.42.71

Castresana J (2000) Selection of conserved blocks from multiple alignments for their use in phylogenetic analysis. Molecular Biology and Evolution, 17(4): 540–552. https://doi.org/10.1093/oxfordjournals.molbev.a026334

Fricke R, Eschmeyer WN & Fong JD (2026) Eschmeyer's Catalog of Fishes: genera/species by family/subfamily. http://researcharchive.calacademy.org/research/ichthyology/catalog/SpeciesByFamily.asp (Accessed 23 June 2026).

Henninger G (1908) Die Labyrinthorgane bei Labyrinthfischen. Zoologische Jahrbücher, Abteilung für Anatomie 25 (for 1907), 251–304.

Hyrtl J (1863) Über eine neue Rippenart und über ds Labyrinth von *Polyacanthus hasselti*. Denkschriften der kaiserlichen Akademie der Wissenschaften, Naturwissenschaftliche Klasse, 21: 11–16.

Freyhof J & Herder F (2002) Review of the paradise fishes of the genus *Macropodus* in Vietnam, with description of two new species from Vietnam and southern China (Perciformes: Osphronemidae). Ichthyological Exploration of Freshwaters, 13(2): 147–167.

Katoh K & Standley DM (2013) MAFFT Multiple Sequence Alignment Software version 7: Improvements in performance and usability. Molecular Biology and Evolution, 30(4): 772–780. https://doi.org/10.1093/molbev/mst010

Kottelat M (1991) Notes on the taxonomy and distribution of some western Indonesian freshwater fishes, with diagnoses of a new genus and six new species (Pisces: Cyprinidae, Belontiidae, and Chaudhuriidae). Ichthyological Exploration of Freshwaters, 2(3): 273–287.

Kottelat M (2013) The fishes of the inland waters of southeast Asia: a catalogue and core bibliography of the fishes known to occur in freshwaters, mangroves and estuaries. Raffles Bulletin of Zoology, Supplement 27: 1–663.

Lemoine F, Correia D, Lefort V, Doppelt-Azeroual O, Mareuil F, Cohen-Boulakia S & Gascuel O (2019) NGPhylogeny.fr: new generation phylogenetic services for non-specialists. Nucleic Acids Research, 47(W1): W260–W265. https://doi.org/10.1093/nar/gkz303

Liem KF (1961) The comparative osteology and phylogeny of the Anabantoidei, with a proposal of a new order Luciocephaliformes. Unpublished PhD Thesis. University of Illinois, Ann Arbor, Michigan, USA, 376 pp.

Liem KF (1963) The comparative osteology and phylogeny of the Anabantoidei (Teleostei, Pisces). Illinois Biological Monographs, 30: 1–149. https://doi.org/10.5962/bhl.title.50281

Liem KF (1965) The status of the anabantoid fish genera *Ctenops* and *Trichopsis*. Copeia, 1965: 206–213. https://doi.org/10.2307/1440725

Liem KF (1967a) A morphological study of *Luciocephalus pulcher*, with notes on gular elements in other recent teleosts.

Journal of Morphology, 121: 103–134. https://doi.org/10.1002/jmor.1051210203

Liem KF (1967b) Functional morphology of the head of the anabantoid teleost fish *Helostoma temmincki*. Journal of Morphology, 121: 135–158. https://doi.org/10.1002/jmor.1051210204

Liem KF (1980) Air ventilation in advanced teleosts: biomechanical and evolutionary aspects. In: Ali MA (ed.) Environmental Physiology of Fishes. Plenum Press, New York, pp. 57–91.

Minh BQ, Schmidt HA, Chernomor O, Schrempf D, Woodhams MD, Haeseler A von & Lanfear R (2020) IQ-TREE 2: New models and efficient methods for phylogenetic inference in the genomic era. Molecular Biology and Evolution, 37(5): 1530–1534. https://doi.org/10.1093/molbev/msaa015

Norris SM & Teugels GG (1990) A new species of *Ctenopoma* (Teleostei: Anabantidae) from southeastern Nigeria. Copeia, 1990(2): 492–499. https://doi.org/10.2307/1446353

Peters HM (1978) On the mechanism of air ventilation in anabantoids (Pisces: Teleostei). Zoomorphologie, 89: 93–123. https://doi.org/10.1007/BF00995663

Roberts TR (1992) Systematic revision of the southeast Asian anabantoid fish genus *Osphronemus*, with descriptions of two new species. Ichthyological Exploration of Freshwaters, 2(4): 351–360.

Rüber L, Britz R & Zardoya R (2006) Molecular phylogenetics and evolutionary diversification of labyrinth fishes (Perciformes: Anabantoidei). Systematic Biology, 55(3): 374–397. https://doi.org/10.1080/10635150500541664

Rüber L, Gandolfi A, Foresti D, Paltrinieri L, Splendiani A & Seehausen O (2023) Phylogenetic and biogeographic history of brook lampreys (*Lampetra*: Petromyzontidae) in the river basins of the Adriatic Sea based on DNA barcode data. Ecology and Evolution, 13(9): e10496. https://doi.org/10.1002/ece3.10496

Skelton PH, Stauffer JR Jr, Chakona A & Wisor JM (2021) Two new species of African bubble-nesting *Microctenopoma* (Teleostei: Anabantidae) from Angola. Ichthyological Exploration of Freshwaters, 30(4): 345–360.

Swofford DL (2002) Phylogenetic Analysis Using Parsimony (*and other methods). Version 4. Sinauer Associates, Sunderland, Massachusetts, 144 pp.

Weitzman SH & Vari RP (1988) Miniaturization in South American freshwater fishes; an overview and discussion. Proceedings of the Biological Society of Washington, 101: 444–465.